Waves in central fields. Scattering of alpha particles from nuclei

Author: Laia Barjuan Ballabriga
Facultat de Física, Universitat de Barcelona, Diagonal 645, 08028 Barcelona, Spain.

Advisor: Dr Francesc Salvat Pujol

Abstract: The quantum problem of a particle in a central field of force has been studied. A robust numerical algorithm has been utilized for solving the radial wave equation for both bound and free states. The general expression of distorted waves has been employed in calculations of elastic scattering of alpha particles from nuclei. The absorptive effect of the imaginary component of the optical-model potential has been analyzed.

I. INTRODUCTION

The present work was mostly performed during the summer of 2019 at CERN, while I was a Summer Student under the supervision of Dr Francesc Salvat Pujol. The aim of the project was to get introduced into the field of Monte Carlo simulation of radiation transport and, in particular, to theoretical calculations of elastic collisions of alpha particles with nuclei [1]. My host group was studying this process in order to refine its description in FLUKA, a fully integrated Monte Carlo simulation package of radiation transport.

I learnt to solve the Schrödinger equation for arbitrary central potentials by using the RADIAL subroutine package [2], which has been published recently as an update of the original subroutines developed twenty-five years ago. I analyzed Schrödinger bound states, the physical meaning of optical-model potentials, and delved into the study of alpha scattering. Back in Barcelona I complemented the work done at CERN and wrote the present report under the advice of Dr Francesc Salvat Gavaldà.

In elastic scattering the incoming particle bounces off the potential of the target nucleus leaving the latter in its ground state. This process has a prominent effect on the angular spread of particle showers. In my calculations the interaction has been modelled as a phenomenological potential. The quantity that has been calculated is the differential cross section, which describes the probability distribution of the scattering angles and can be measured experimentally.

II. RADIAL

The Fortran subroutine package RADIAL is capable of solving the radial Schrödinger and Dirac wave equations for arbitrary central potentials given in numerical form. The potential function, $rV(r)$, is assumed to be finite for all r and tending to a constant value at large radii. RADIAL approximates the tabulated potential with a cubic spline and integrates the radial equation using a power-series expansion method. The local series are summed up to the prescribed accuracy so that truncation errors are avoided [2]. The subroutines calculate radial wavefunctions, eigenvalues for bound states, and phase shifts for free states for both real potentials and complex optical potentials. These subroutines are flexible, robust, and highly accurate. An advantage of RADIAL is that it can determine whether a particular bound state exists or not. In addition, the grid in which the wavefunction is calculated and the grid where the potential is tabulated are completely independent of each other. The RADIAL subroutines have been thoroughly tested and have been used not only by the authors but also by other research groups to solve a wide variety of problems.

III. BOUND STATES

I solved the Schrödinger equation for bound states of nucleons in the spirit of the shell model. Shortly, the shell model considers that neutrons and protons fill their corresponding single particle bound states, in order of increasing energy consistently with the Pauli principle, similarly to what is done with electrons in atomic physics. Thus, one obtains an inert core of completely filled shells and some weakly bound nucleons that determine relevant nuclear properties. When all major shells are filled and no additional nucleons are left, relatively wide gaps between energy levels appear. These gaps always occur after allocating the same numbers of protons or neutrons, the "magic numbers" (2, 8, 20, 28, 50, 82 and 126) [3].

The first step in developing the shell model is the choice of an appropriate phenomenological potential, which is intended to reproduce the essential features of a realistic nuclear potential. The parameters used are chosen in order to improve the agreement between the calculations and the body of available experimental data. Here I used a phenomenological potential of the kind described below kindly provided by Dr Xavier Viñas.

The potential is expressed as the sum of the Coulomb potential of a homogeneously charged sphere, $V_{\rm C}(r)$, a real modified Woods-Saxon term, $V_{\rm R}(r)$, and a spin-orbit term, $V_{\rm SO}(r)$,

$$V(r) = V_{\rm C}(r) + V_{\rm R}(r) + V_{\rm SO}(r)(\vec{\sigma}\cdot\vec{\ell}), \tag{1}$$

where

$$V_{\rm R}(r) = V_{\rm R}[f(R_{\rm R}, a_{\rm R}; r)]^{\nu_{\rm R}}, \tag{2}$$

$$V_{\rm SO}(r) = U_{\rm SO}\frac{\rm d}{{\rm d}r}\{[f(R_{\rm SO}, a_{\rm SO}; r)]^{\nu_{\rm SO}}\}, \tag{3}$$

and the Woods-Saxon factor is

$$f(R_i, a_i; r) = \frac{1}{1 + \exp\left[(r - R_i)/a_i\right]}. \quad (4)$$

The parameters $V_{\rm R}$, $U_{\rm SO}$ and R_i, the nuclear radius, depend on the mass number, A, and on the asymmetry parameter, $I = (N - Z)/A$. The diffuseness parameter, a_i, also depends on I. Additionally, these parameters, $\nu_{\rm R}$, and $\nu_{\rm SO}$ are specific of the type of nucleon.

I wrote a program which uses the RADIAL subroutines to compute all the possible bound energy levels for neutrons or protons using the potential described in Eq. (1). I computed the energy levels by sweeping the principal quantum numbers up to 10 and their corresponding angular momentum quantum numbers, ℓ, for the potentials without and with spin-orbit term.

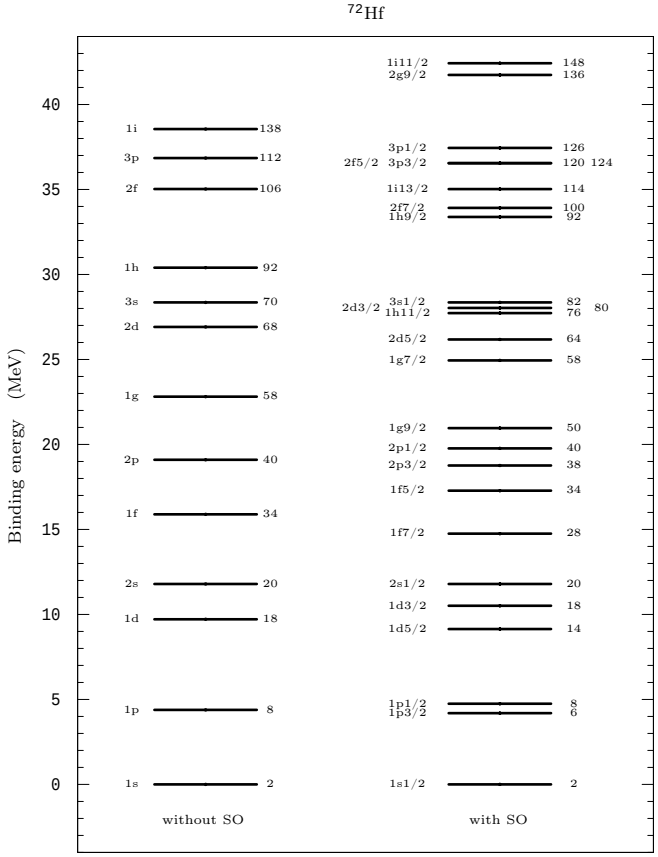

FIG. 1: Calculated neutron energy levels of ^{72}Hf from the phenomenological potential. The left column displays energy levels calculated without the spin-orbit term. Spectroscopic notation is used except for the fact that the index n counts the number of levels with that ℓ [3]. To the right of each level, the cumulative number of nucleons is shown. The right column displays the energy levels calculated with spin-orbit interaction.

Figure 1 displays the energy levels of ^{72}Hf obtained from RADIAL. Shell model predictions with optical potentials are purely qualitative and are not expected to numerically coincide with the experimental values. That notwithstanding, when the spin-orbit term is added, the energy levels rearrange so that the gaps between states correspond to the correct magic numbers.

IV. ELASTIC SCATTERING

Let us study the scattering of non-relativistic particles from nuclei. The interaction is through a potential assumed to depend only on the relative distance between the projectile and the nucleus. In the calculations I adopted the stationary-state approximation.

The Schrödinger Hamiltonian splits into two terms. The first one corresponds to the center of mass motion and the second one describes the motion of the projectile relative to the nucleus. Thus, the original two-body problem is decoupled into two one-body problems [4]. I henceforth will work in the center of mass frame, in which the Schrödinger equation for the relative motion reads

$$-\frac{\hbar^2}{2\mu}\nabla^2 + V(r) \quad \psi(\vec{r}) = E\psi(\vec{r}), \quad (5)$$

where μ is the reduced mass of the two particles. In scattering problems one looks for free (unbound) solutions with energy $E = \vec{p}^{\,2}/2\mu$ and relative momentum $\vec{p} = \hbar\vec{k}$.

Although I focused on the elastic scattering of alpha particles, I also had a look to neutron scattering. To describe the interaction, I used optical-model potentials.

A. Optical-model potentials

Optical-model potentials account for the electrostatic and strong forces experienced by the projectile, a hadron or a light nucleus, in the vicinity of a target nucleus. They consist of various terms with parameters that have been adjusted to optimize the overall fit to the available experimental data, within a given range of energies and mass numbers of the target nucleus. For scattering of alpha particles I used the parametrization of Su *et al.* [5] which is intended for target mass numbers $20 \leq A \leq 209$ and energies of the alpha particle up to 386 MeV.

The interaction potential between the target nucleus and the alpha particle is represented as the sum of the electrostatic potential of a homogeneously charged sphere, $V_{\rm C}(r)$, a real central term of Woods-Saxon form, $V_{\rm R}(r, E)$, and an absorptive potential, $W(r, E)$, which consists of a Woods-Saxon volume term, $W_V(r, E)$, and a term peaked at the nuclear surface, $W_S(r, E)$,

$$V(r, E) = V_{\rm C}(r) + V_{\rm R}(r, E) + {\rm i}[W_{\rm V}(r, E) + W_{\rm S}(r, E)], \quad (6)$$

where

$$V_{\rm R}(r, E) = -V_{\rm R}(E) f(R_{\rm R}, a_{\rm R}; r), \quad (7)$$

$$W_{\rm V}(r, E) = -W_{\rm V}(E) f(R_{\rm V}, a_{\rm V}; r), \quad (8)$$

$$W_{\rm S}(r, E) = -W_{\rm S}(E) \frac{\rm d}{{\rm d}r}[f(R_{\rm S}, a_{\rm S}; r)]. \quad (9)$$

The global factors $V_{\rm R}(E), W_{\rm V}(E)$ and $W_{\rm S}(E)$ depend on the atomic number, Z, the mass number, A, and the projectile energy. The nuclear radii are expressed as $R_i = r_i A^{1/3}$. The quantities a_i and r_i are parameters of the model.

The imaginary absorption potential deserves a specific comment. Aside from elastic scattering, the projectile can undergo inelastic collisions that cause the excitation of the nucleus and an additional energy loss by the projectile. In these interactions the projectile is removed from the elastically scattered wave. This effect is accounted for by introducing an imaginary term, $W(r)$, in the potential. The Schrödinger equation then reads

$$\mathrm{i}\tilde{\hbar}\frac{\partial\Psi(\vec{r},t)}{\partial t} = \frac{-\tilde{\hbar}^2}{2M}\nabla^2\Psi(\vec{r},t) + [V_{\rm R}(r) - \mathrm{i}W(r)]\Psi(\vec{r},t), \tag{10}$$

where $V_{\rm R}(r)$ is the real part of the potential. Considering the probability density

$$\rho = |\Psi(\vec{r},t)|^2 \tag{11}$$

and the current density

$$j(\vec{r},t) = \frac{\tilde{\hbar}}{2M\mathrm{i}}[\Psi^*(\vec{r},t)\vec{\nabla}\Psi(\vec{r},t) - (\vec{\nabla}\Psi^*(\vec{r},t))\Psi(\vec{r},t)], \tag{12}$$

one obtains the continuity equation

$$\frac{\partial\rho}{\partial t} + \vec{\nabla}\cdot j(\vec{r},t) = -\frac{2W(r)}{\tilde{\hbar}}\rho. \tag{13}$$

We thus see that the imaginary term in the potential determines the probability of absorption of the projectile per unit time [6].

B. Distorted waves

In absence of an interaction potential, the solution of the Schrödinger equation (5) is a plane wave, which can be expressed by means of the Rayleigh's expansion

$$\psi(\vec{r}) = 4\pi\sum_{\ell=0}^{\infty}\mathrm{i}^\ell j_\ell(kr)\sum_{m=-\ell}^{\ell}Y_{\ell m}(\vec{r})Y^*_{\ell m}(\vec{k}), \tag{14}$$

where $j_\ell(kr)$ are the spherical Bessel functions and $Y_{\ell m}(\vec{r})$ are the spherical harmonics.

When the interaction potential is considered, the required solutions of the Schrödinger equation are the distorted plane waves (DPW). That is, exact solutions that when the distorting potential is adiabatically removed reduce to the plane waves. For the sake of simplicity, I assume a finite range potential. For such potential, the DPW can be written as [4]

$$\psi^{(\pm)}_{\vec{k}}(\vec{r}) = \frac{4\pi}{kr}\sum_{\ell=0}^{\infty}\mathrm{i}^\ell\exp(\pm\mathrm{i}\delta_\ell)P_{E\ell}(r)\sum_{m=-\ell}^{\ell}Y_{\ell m}(\vec{r})Y^*_{\ell m}(\vec{k}), \tag{15}$$

where $P_{E\ell}$ are the free (positive energy) solutions of the radial equation

$$\frac{-\tilde{\hbar}^2}{2\mu}\frac{\mathrm{d}^2}{\mathrm{d}r^2} + \frac{\tilde{\hbar}^2}{2\mu}\frac{\ell(\ell+1)}{r^2} + V(r)\;\; P_{E\ell}(r) = EP_{E\ell}(r), \tag{16}$$

with the asymptotic behaviour

$$P_{E\ell}(r) \underset{r\to\infty}{\sim} \sin\;\; kr - \frac{\ell\pi}{2} + \delta_\ell \quad , \tag{17}$$

which determines their normalization.

From the properties of spherical harmonics (addition theorem) and the asymptotic behaviour of the radial functions, one obtains that the DPW asymptotically behaves as

$$\psi^{(\pm)}_{\vec{k}}(\vec{r}) \underset{r\to\infty}{\sim} A\;\; \exp(\mathrm{i}\vec{k}\vec{r}) + f(\hat{r})\frac{\exp(\pm\mathrm{i}\vec{k}\vec{r})}{r} \quad , \tag{18}$$

where

$$f(\hat{r}) = \frac{1}{2\mathrm{i}k}\sum_{\ell=0}^{\infty}[(2\ell+1)P_\ell(\vec{k}\cdot\vec{r})(\exp(2\mathrm{i}\delta_\ell) - 1)] \tag{19}$$

is the scattering amplitude and $P_\ell(\vec{k}\cdot\vec{r})$ are the Legendre polynomials. Note that the asymptotic DPW reduces to a plane wave plus an outgoing (+) or incoming (-) spherical wave. This character is clearly seen once the time dependence is introduced into the stationary state, $\Psi^{(\pm)}_{\vec{k}}(\vec{r},t) = \psi^{(\pm)}_{\vec{k}}(\vec{r})\exp(-\mathrm{i}Et/\tilde{\hbar})$. Figure 2 is a screenshot of an animation generated with gnuplot that shows the time evolution of a DPW with outgoing spherical component.

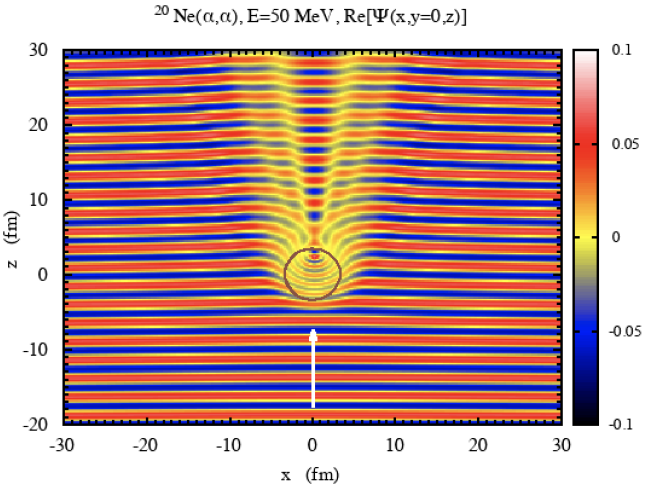

FIG. 2: Real part of the DPW, $\Psi^{(+)}_{\vec{k}}(\vec{r};t)$, for 50 MeV alpha particles impinging on ^{20}Ne along the direction of the white arrow. The brown circle represents the position and radius of the target nucleus.

In scattering experiments, the quantity measured experimentally is the differential cross section (DCS). It is defined as the ratio of the flux of the outgoing scattered particles, $j_{\rm out}$, and the flux of the incoming ones, $j_{\rm in}$. Measurements of the DCS are performed at very

large distances from the scattering center. Therefore, the wave that reaches the detector is determined by the asymptotic behaviour of the radial functions, Eq. (17), where the effect of the interaction is summarized in the phase shift.

From Eqs. (12) and (18) one concludes that the DCS is

$$\frac{\mathrm{d}\sigma}{\mathrm{d}\Omega} = \frac{\mathrm{d}j_{\mathrm{out}}}{j_{\mathrm{in}}\mathrm{d}\Omega} = |f(\hat{r})|^2. \tag{20}$$

Hence, to calculate the DCS one has to select the alpha-nucleus potential, solve the Schrödinger equation for the different values of ℓ, and obtain the phase shifts. Once the phase shifts are known, the calculation of the DCS is straightforward.

The RADIAL subroutines solve the Schrödinger radial equation calculating the radial functions up to a large enough radius. At this radius, the phase shifts are determined by matching the radial function to a combination of Bessel and Neumann functions.

It is worth noticing that the previous discussion applies only to finite-range potentials, while in the scattering of alpha particles the projectile also feels the long-range Coulomb potential. In this case, one could calculate the total phase shift due to the combined Coulomb and short-range potentials. However, the partial-wave series of the scattering amplitude would converge very slowly. A method to speed up the convergence of this series, is to add the Coulomb scattering amplitude and subtract its partial-wave series, both of them known analitically. In this way, the resulting series converges as rapidly as that of the short-range potential alone. Naturally, in this case the relevant phase shifts are those of the short-range potential only. RADIAL computes them by matching the calculated radial functions to a combination of Coulomb functions [2].

To isolate the spherical part of the DPW, I consider the scattering of neutrons for which the potential is of short range. In this case, one can isolate the scattered wave by subtracting from the DPW the asymptotic plane wave. At large distances, the scattered wave is correlated to the DCS by means of Eq. (20). For neutrons, I have used the default optical-model potential provided in the RADIAL package [7]. The correspondence between the scattered wave and the DCS is clearly visible in Figs. 3 and 4.

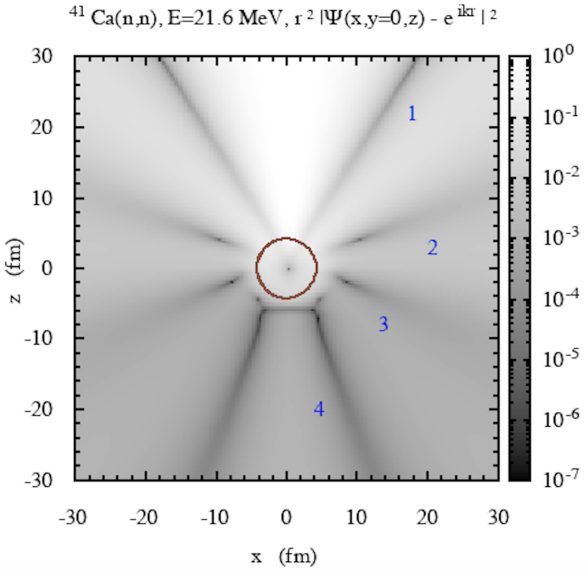

FIG. 3: Squared modulus of the scattered wave for a 21.6 MeV neutron beam impinging on ^{41}Ca. The numbers label the four minima observed, the target nucleus is represented by the brown circle.

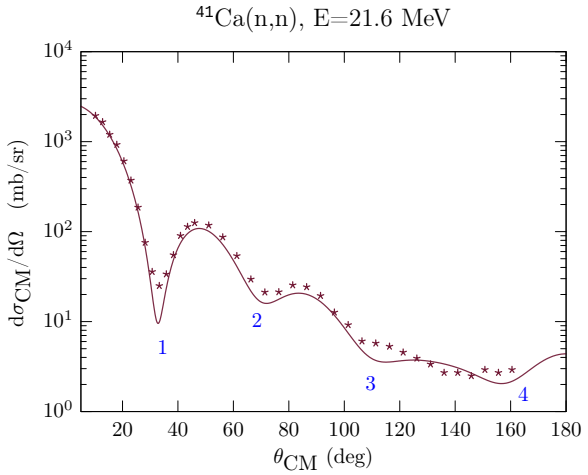

FIG. 4: DCS for a 21.6 MeV neutron beam impinging on ^{41}Ca. The numbers label the minima that correlate with the structures in Fig. 3. Experimental data are from the EXFOR database [8].

C. Theoretical calculations and assessment

I have examined the results of calculations of elastic scattering of alpha particles for the targets ^{20}Ne, ^{58}Ni and ^{90}Zr, using the experimental data available in the EXFOR database [8], since the chosen potential model is expected to cover these cases.

Figure 5 compares the calculated DCSs for these target nuclei with the experimental data. Overall, the agreement is satisfactory. Although for large scattering angles and energies it is more questionable, one must keep in mind that I have used a global phenomenological optical model, *i.e.* its parameters are fitted to approach the main features of the experimental data (such as the slope or the position of the minima) for as many targets as possible. To obtain a more accurate description one should use local-model potentials with parameters fitted to reproduce specific cases. In addition, there is even considerable discrepancy between different sets of experimental data for the same target and the same energy of the projectile. Therefore, one can conclude that the results from the present calculations are satisfactory.

FIG. 5: Calculated DCSs (curves) compared with experimental data (symbols) for three different target nuclei and the indicated energies. The top curves and data points represent actual values, while the other sets are offset by factors of 10 ^{3}.

V. CONCLUSIONS

As a result of this project I broadened my knowledge of the quantum mechanics of particles in central fields. I used the RADIAL subroutines to solve the Schrödinger equation for the shell model of the nucleus showing that with an appropiate potential model, and including a spin-orbit term, the magic numbers are obtained. In addition, I studied the elastic scattering of alpha particles from nuclei and I analyzed the structure and time evolution of DPWs. Finally, with the adopted optical-model potential and using the elementary stationary-state treatment of scattering processes, I verified that the calculation results are in good agreement with experimental data.

The developed code for elastic collisions of alpha particles with nuclei will be used to generate a database of DCSs to be implemented in Monte Carlo simulations of alpha particle transport.

Acknowledgments

I am thankful to Dr Francesc Salvat Pujol who hosted me at CERN as a Summer Student and patiently guided me in my first contact with the world of research while instructing me in this particular field. I am also indebted to Dr Francesc Salvat Gavaldà for his guidance during the development of this work and his advice all this time. Finally, I also want to express my gratitude to my parents who have always boosted me to pursue a scientific career and for their unconditional support.

[1] L. Barjuan, *Generation of a database of di erential cross sections for nuclear elastic scattering of particles on nuclei*, CERN-STUDENTS-Note-2019, No. 120. http://cds.cern.ch/record/2687379

[2] F. Salvat and J.M. Fernández-Varea,"RADIAL: a Fortran subroutine package for the solution of the radial Schrödinger and Dirac wave equations." *Comput. Phys. Commun.* **240** (2019): 165-177.

[3] K.S.Krane, *Introductory Nuclear Physics*, 2nd ed., (John-Wiley and Sons, New York, 1988).

[4] C. Joachain, *Quantum collision theory*, (North-Holland Publishing Company, New York, 1975).

[5] X.W. Su and Y.L. Han, "Global optical model potential for alpha projectile", *Int. J. Mod. Phys.*, **24**, No. 12 (2015).

[6] L.I. Schiff, *Quantum Mechanics*, 3rd ed., (McGraw-Hill Book Company, New York, 1968), pp 129-130.

[7] A.J. Koning and J.P. Delaroche, "Local and global nucleon optical models from 1 keV to 200 MeV." *Nucl. Phys. A* **713** (2003): 231–310.

[8] EXFOR database. https://www-nds.iaea.org/exfor/